The Meteoritical Society

Meteoritics & Planetary Science 43, Nr 5, 941–958 (2008)
Abstract available online at http://meteoritics.org

A study of ordinary chondrites by Mössbauer spectroscopy with high-velocity resolution

M. I. OSHTRAKH[1*], E. V. PETROVA[1], V. I. GROKHOVSKY[1], and V. A. SEMIONKIN[2]

[1]Faculty of Physical Techniques and Devices for Quality Control, Ural State Technical University-UPI, Mira str. 19, Ekaterinburg 620002, Russia
[2]Faculty of Experimental Physics, Ural State Technical University-UPI, Ekaterinburg 620002, Russian Federation
*Corresponding author. E-mail: oshtrakh@mail.utnet.ru

(Received 13 February 2007; revision accepted 21 November 2007)

Abstract–An improvement in the velocity resolution and quality of Mössbauer spectra has been applied to a group of ordinary chondrites. This improvement permitted us to carry out a more detailed study of the iron bearing phases in these samples than has previously been possible. Mössbauer spectra of 11 ordinary chondrites of L and H chemical groups were measured using 4096 channels and presented for further analysis in 1024 channels. Subspectra of the metal grains of several chondrites demonstrated the presence of at least two magnetic sextets related to the main Fe(Ni, Co) phases. Moreover, Mössbauer study of extracted metal grains from Tsarev L5 revealed three sextets and one singlet spectral components related to various α-Fe(Ni, Co), α′-Fe(Ni, Co), α_2-Fe(Ni, Co), and γ-Fe(Ni, Co) phases. Each subspectrum of olivine and pyroxene in Mössbauer spectra of ordinary chondrites was fitted by superposition of two quadrupole doublets related to M1 and M2 sites in minerals for the first time. An analysis of relative areas and Mössbauer hyperfine parameters was performed and some differences for L and H chondrites as well as for M1 and M2 sites were observed. Mössbauer parameters of troilite and oxidized iron were analyzed. In contrast to a previous study with 512-channel spectra, the presence of oxidized iron was found in all chondrites.

INTRODUCTION

Mössbauer spectroscopy is a useful tool for studying meteorites, in particular, ordinary chondrites to analyze their chemical and phase composition. Iron-bearing phases in ordinary chondrites olivine $(Fe, Mg)_2SiO_4$, pyroxene (Fe, Mg, Ca)SiO_3, troilite (FeS), and metal (Fe-Ni-Co alloys) as well as its weathering products can be identified and characterized by ^{57}Fe Mössbauer spectroscopy. Ordinary chondrites contain 19–28 wt% of total Fe, including 2–17 wt% of Fe in metal, 4–6 wt% of Fe in troilite and 10–18 wt% of Fe in silicates (Jarosewich 1990). Ordinary chondrites are related to three groups: H, L, and LL. These groups are characterized by different total iron content and different metal iron content. The content of metal iron in H, L, and LL groups of ordinary chondrites is 15–19 wt%, 4–10 wt%, and 1–3 wt%, respectively. These groups contain a weight percentage of total Fe from 25 to 28%, from 20 to 25%, and from 19 to 22%, as well as different ranges of fayalite (Fa): 16–20 mol%, 22–26 mol%, and 27–31 mol% for H, L, and LL groups, respectively (Dodd 1981). Therefore, Mössbauer spectroscopy was applied in various studies of ordinary chondrites (for instance, Sprenkel-Segel and Hanna 1964; Danon et al. 1979; de Oliveira et al. 1988; Ortalli and Pedrazzi 1990; Gismelseed et al. 1994, 2005; Zhang et al. 1994; Bland et al. 1996, 1998a, 1998b; Abdu and Ericsson 1997; Dunlap 1997; Scorzelli et al. 1998; Grandjean et al. 1998; Calogero et al. 1999; Paliwal et al. 2000; Verma et al. 2002, 2003, 2004; Menzies et al. 2005; Al-Rawas et al. 2007).

Metal grains in ordinary chondrites may contain various phases such as α-Fe(Ni, Co) or kamacite, with Ni content up to 7.5 wt%, α_2-Fe(Ni, Co)-distorted phase supersaturated in Ni, so-called martensite with Ni content in the range of ~15–25 wt%, α′-Fe(Ni, Co), secondary kamacite resulted from decomposition of α_2-Fe(Ni, Co), with Ni content in the range of ~7–15 wt%, and γ-Fe(Ni, Co) or taenite, with Ni content in the range of 25–45 wt%. However, low content of total metal, and especially lower partial content of each Fe-Ni-Co phase in ordinary chondrites, complicates the determination of its phase composition from Mössbauer spectra. Earlier, the presence of ~7% of kamacite and ~2% of tetrataenite (ordered γ-Fe(Ni, Co) phase) was found in New Halfa meteorite by Mössbauer spectroscopy (Abdu and Ericsson 1997). Visual evaluation of symmetry of the most negative velocity

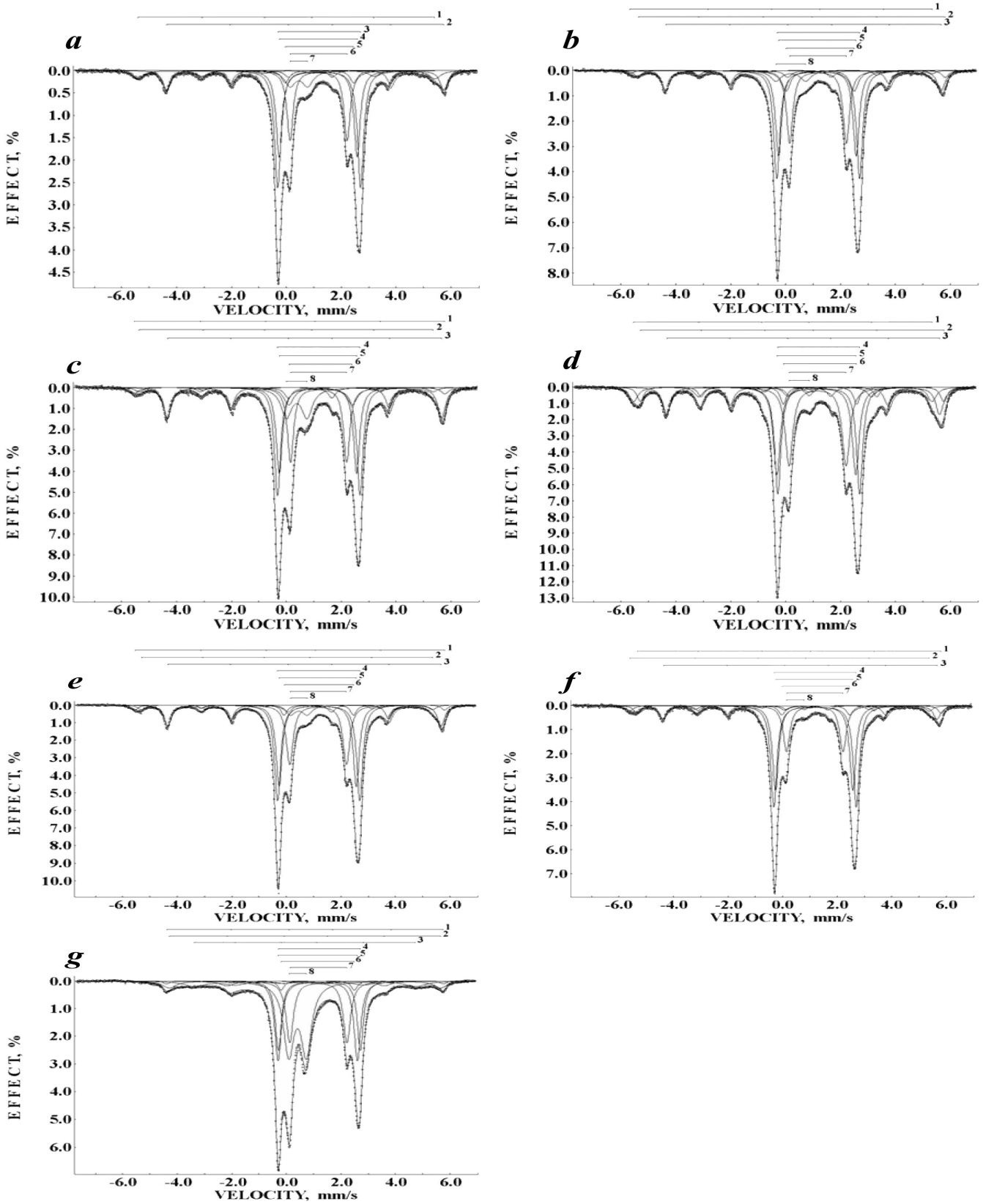

Fig. 1. Mössbauer spectra of ordinary chondrites (chemical group L): a) Saratov L4. b) Mount Tazerzait L5. c) Tsarev L5. d) Farmington L5. e) Mbale L5/6. f) Kunashak L6. g) Zubkovsky L6. Components are given in Table 1. T = 295 K.

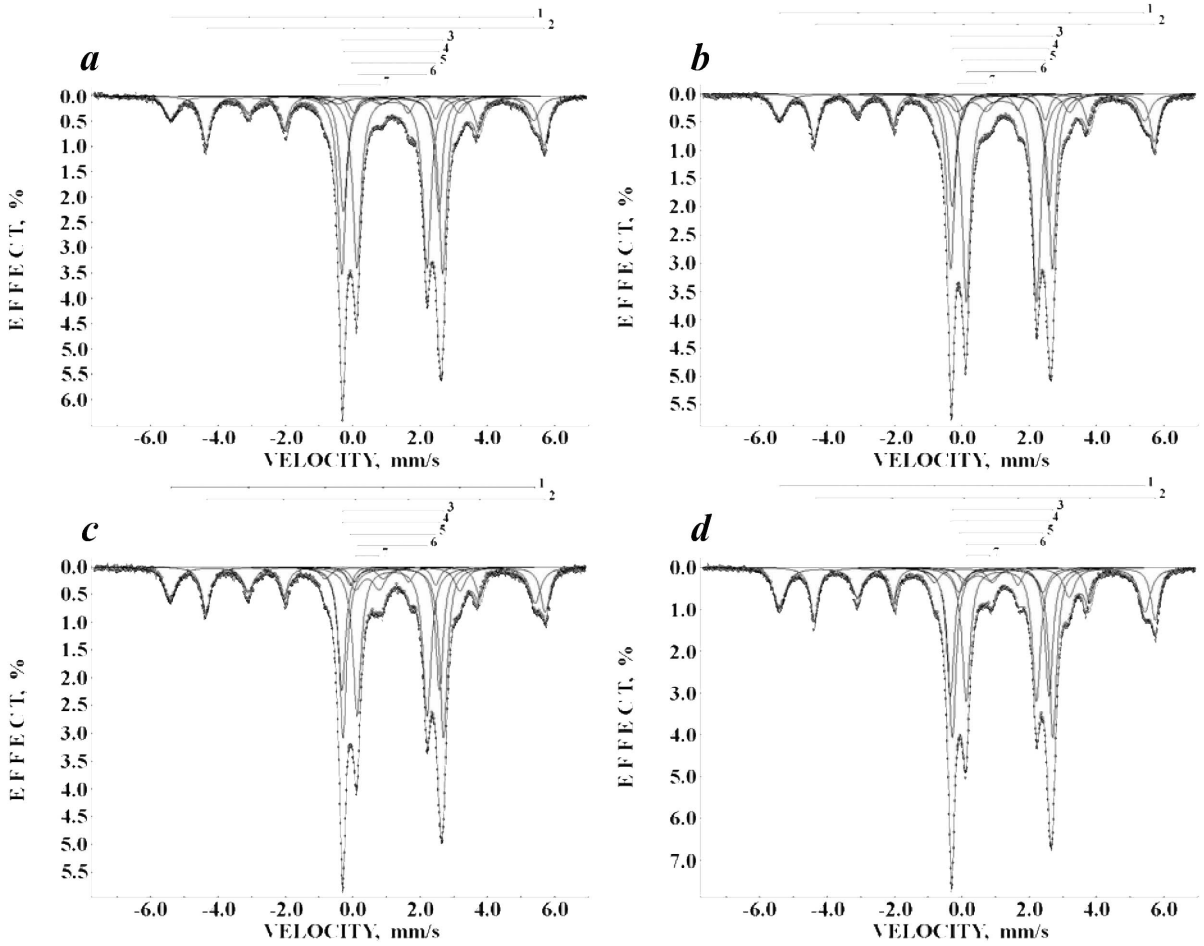

Fig. 2. Mössbauer spectra of ordinary chondrites (chemical group H). a) Ochansk H4. b) Richardton H5. c) Vengerovo H5. d) Zvonkov H6. Components are given in Table 1. T = 295 K.

absorption peak was used to determine the presence of taenite contribution (Verma et al. 2002). Recently, 512 channels Mössbauer spectra measurements of ordinary chondrites using spectrometer with high-velocity resolution revealed asymmetry of sextets related to metal grains in some ordinary chondrites. These spectral components were fitted by superposition of two sextets related to different Fe(Ni, Co) phases (Zhiganova et al. 2005). Extraction of metal or magnetic parts from ordinary chondrites was another way to study metal grains and their phase composition (Danon et al. 1979; Scorzelli et al. 1994, 1998; Kong et al. 1995; Kong and Ebihara 1996; Bahgat et al. 2000; Ludwig et al. 2001; Abdu et al. 2002).

It is well known that both olivine and pyroxene contain two crystallographically non-equivalent six-fold octahedral sites for Fe^{2+} and Mg^{2+} denoted as M1 and M2. These sites in olivine and pyroxene are occupied by Fe^{2+} and Mg^{2+} ions in different ways. The Fe-Mg distribution between two sites is of interest due to its possible application for determination of the minerals cooling history. The contrast of M1 and M2 sites geometry in olivine is less than that in pyroxene. Mössbauer spectroscopy was successfully used to distinguish M1 and M2 sites in pure synthetic and natural orthopyroxenes (Pasternak et al. 1992; Van Alboom et al. 1993; Wang et al. 2005; Dyar et al. 2007), clinopyroxenes (Eeckhout et al. 2000; De Grave and Eeckhout 2003a, 2003b), and olivines (Morozov et al. 2005a, 2005b). Nevertheless, there were no attempts to distinguish subspectra related to M1 and M2 sites in both olivine and pyroxene in Mössbauer spectra of ordinary chondrites except the study of extracted silicates (Gismelseed et al. 2004).

In the present work, the possibilities of Mössbauer spectroscopy with high-velocity resolution were considered on the basis of 11 ordinary chondrites from H and L groups study after the first preliminary results (Oshtrakh and Zhiganova 2006; Zhiganova and Oshtrakh 2006; Zhiganova et al. 2007).

EXPERIMENTAL METHODS

Equilibrated ordinary chondrites from H and L chemical groups Saratov L4, Mount Tazerzait L5, Tsarev L5,

Table 1. Mössbauer parameters of ordinary chondrites.

Sample	Γ^a (mm/s)	δ^b (mm/s)	$\Delta E_Q{}^b$ (mm/s)	$H_{eff}{}^c$ (kOe)	S (%)	Compound[d]
Saratov	0.491	0.031	–0.057	335.6	7.71	Fe(Ni, Co) (1)
L4	0.337	0.779	–0.182	313.5	12.29	FeS (2)
	0.270*	1.193	3.022	–	29.67	Olivine M1 (3)
	0.270*	1.158	2.840	–	21.97	Olivine M2 (4)
	0.326	1.207	2.491	–	3.80	Pyroxene M1 (5)
	0.274	1.173	2.080	–	17.96	Pyroxene M2 (6)
	0.473	0.454	0.642	–	6.60	Fe^{3+} (7)
Mount	0.290*	0.103	–0.541	342.0	1.79	Fe(Ni, Co) (1)
Tazerzait	0.300*	0.146	0.146	347.4	3.94	Fe(Ni, Co) (2)
L5	0.345	0.762	–0.219	311.3	13.08	FeS (3)
	0.270*	1.189	3.016	–	27.81	Olivine M1 (4)
	0.270*	1.159	2.830	–	22.04	Olivine M2 (5)
	0.370	1.260	2.479	–	7.30	Pyroxene M1 (6)
	0.280	1.181	2.065	–	19.35	Pyroxene M2 (7)
	0.472	0.188	1.088	–	4.70	Fe^{3+} (8)
Tsarev	0.347	0.129	–0.032	351.3	3.54	Fe(Ni, Co) (1)
L5	0.351	0.028	–0.077	333.0*	2.49	Fe(Ni, Co) (2)
	0.338	0.763	–0.202	310.0	16.99	FeS (3)
	0.270*	1.180	3.007	–	23.89	Olivine M1 (4)
	0.270*	1.150	2.819	–	19.00	Olivine M2 (5)
	0.443	1.241	2.308	–	6.25	Pyroxene M1 (6)
	0.274	1.174	2.048	–	16.73	Pyroxene M2 (7)
	0.472	0.376	0.754	–	11.11	Fe^{3+} (8)
Farmington	0.286	0.180	0.115	343.1	6.51	Fe(Ni, Co) (1)
L5	0.385	–0.059	–0.083	337.6	8.71	Fe(Ni, Co) (2)
	0.348	0.748	–0.217	308.7	14.84	FeS (3)
	0.270*	1.207	2.982	–	22.64	Olivine M1 (4)
	0.303	1.119	2.876	–	20.80	Olivine M2 (5)
	0.270*	1.256	2.672	–	3.63	Pyroxene M1 (6)
	0.337	1.165	2.078	–	20.66	Pyroxene M2 (7)
	0.342**	0.499	0.730*	–	2.22	Fe^{3+} (8)
Mbale	0.270*	0.143	–0.036	352.4	3.04	Fe(Ni, Co) (1)
L5/6	0.330	0.024	–0.003	331.4	3.38	Fe(Ni, Co) (2)
	0.326	0.762	–0.198	310.9	14.75	FeS (3)
	0.270*	1.185	3.014	–	27.97	Olivine M1 (4)
	0.270*	1.149	2.832	–	23.89	Olivine M2 (5)
	0.270	1.191	2.544	–	3.00	Pyroxene M1 (6)
	0.305	1.163	2.080	–	19.56	Pyroxene M2 (7)
	0.435	0.457	0.614	–	4.41	Fe^{3+} (8)
Kunashak	0.273	0.185	0.102	346.2	4.87	Fe(Ni, Co) (1)
L6	0.317	–0.066	–0.090	341.0	4.21	Fe(Ni, Co) (2)
	0.332	0.759	–0.223	311.6	10.56	FeS (3)
	0.271	1.195	3.023	–	32.66	Olivine M1 (4)
	0.270*	1.162	2.836	–	27.18	Olivine M2 (5)
	0.299	1.221	2.485	–	3.27	Pyroxene M1 (6)
	0.291	1.182	2.070	–	15.89	Pyroxene M2 (7)
	0.293	0.471	0.644	–	1.37	Fe^{3+} (8)
Zubkovsky	0.270*	0.789	–0.222	314.6	1.34	FeS (1)
L6	0.600	0.693	–0.030	308.6	6.97	FeS (2)
	0.900*	0.578	0.207	251.7	8.01	Fe^{3+} (mag.) (3)
	0.270*	1.210	3.005	–	16.20	Olivine M1 (4)
	0.295	1.150	2.909	–	20.26	Olivine M2 (5)
	0.270*	1.150	2.685	–	2.14	Pyroxene M1 (6)
	0.320*	1.172	2.097	–	16.98	Pyroxene M2 (7)
	0.462	0.411	0.645	–	28.11	Fe^{3+} (8)

Table 1. *(Continued).* Mössbauer parameters of ordinary chondrites.

Sample	Γ^a (mm/s)	δ^b (mm/s)	$\Delta E_Q{}^b$ (mm/s)	$H_{eff}{}^c$ (kOe)	S (%)	Compound[d]
Ochansk	0.442	0.020	–0.059	334.6	10.72	Fe(Ni, Co) (1)
H4	0.349	0.763	–0.180	311.4	17.39	FeS (2)
	0.275	1.178	3.000	–	24.83	Olivine M1 (3)
	0.270*	1.144	2.834	–	15.84	Olivine M2 (4)
	0.306	1.218	2.502	–	3.53	Pyroxene M1 (5)
	0.292	1.167	2.077	–	25.34	Pyroxene M2 (6)
	0.600*	0.205	1.250	–	2.35	Fe^{3+} (7)
Richardton	0.429	0.035	–0.051	336.6	11.03	Fe(Ni, Co) (1)
H5	0.323	0.770	–0.188	313.5	14.71	FeS (2)
	0.270*	1.182	3.021	–	22.74	Olivine M1 (3)
	0.270*	1.149	2.869	–	14.65	Olivine M2 (4)
	0.280	1.240	2.483	–	3.54	Pyroxene M1 (5)
	0.293	1.178	2.086	–	29.05	Pyroxene M2 (6)
	0.559	0.296	0.872	–	4.28	Fe^{3+} (7)
Vengerovo	0.406	0.023	–0.043	336.5	14.77	Fe(Ni, Co) (1)
H5	0.332	0.776	–0.179	312.6	15.11	FeS (2)
	0.270*	1.208	2.983	–	23.41	Olivine M1 (3)
	0.270*	1.130	2.899	–	16.91	Olivine M2 (4)
	0.283	1.197	2.544	–	2.67	Pyroxene M1 (5)
	0.295	1.170	2.083	–	22.16	Pyroxene M2 (6)
	0.455	0.436	0.708	–	4.98	Fe^{3+} (7)
Zvonkov	0.405	0.032	–0.033	337.0	17.60	Fe(Ni, Co) (1)
H6	0.305	0.778	–0.181	314.0	15.80	FeS (2)
	0.271	1.214	2.988	–	22.61	Olivine M1 (3)
	0.272	1.129	2.931	–	17.19	Olivine M2 (4)
	0.387	1.166	2.478	–	4.82	Pyroxene M1 (5)
	0.288	1.176	2.085	–	18.86	Pyroxene M2 (6)
	0.528	0.491	0.704	–	3.12	Fe^{3+} (7)

[a]Experimental error is ±0.029 mm/s.
[b]ExperImental error is ±0.014 mm/s.
[c]Experimental error is ±0.5 kOe.
[d]Numbers in parenthesis are correspondent to the component numbers in Figs. 1 and 2. *Parameter on bound (limit of variation). **fixed parameter.

Farmington L5, Mbale L5/6, Kunashak L6, Zubkovsky L6, Ochansk H4, Richardton H5, Vengerovo H5, Zvonkov H6 (all chondrites were falls except Zubkovsky L6) were studied in the form of powder and pasted on an Al substrate purified from iron with diameter of 20 mm. The effective thickness of each sample was about 10 mg Fe/cm^2. This value was within the limit of thin absorber, and application of the transmission integral during the fitting was not required (De Grave et al. 1993). Selected chemical analysis of several chondrites was given earlier (Zhiganova et al. 2005). Additionally metal grains extraction from Tsarev L5 was made. Chondrite material was pounded in acetone to prevent metal oxidation on the air and fractional precipitation was made to remove light chondrite components. Then, using hand magnets of varying field strength separation of meteorite particles enriched with metal was made with further pounding of these particles. This procedure was repeated many times to reach maximal metal grains separation from silicates and troilite. To finalize extraction, isolated metal particles were treated with 40% HF solution at room temperature for 20 min to dilute residual silicates and oxidized iron compounds accrete with metal. Metal grains remained non-diluted and got metallic luster. Finally, optical microscope MBI-10M was used to look for the residual silicate particles in the sample. As a result pure metal grains were extracted from chondrite Tsarev L5. To prepare the sample for Mössbauer study 30 mg of extracted metal was pasted on the Al substrate purified from iron with diameter of 20 mm. An effective thickness of the sample was ~10 mg Fe/cm^2. Unfortunately, there was no uniform metal particle distribution on the substrate due to different particle sizes. This further led to a decrease of both absorption effect and the signal/noise ratio.

Mössbauer spectra of the sample powders were measured at room temperature with the constant acceleration computerized high-precision sensitive and stable spectrometer with the saw-tooth velocity reference signal that was a part of multi-dimension parametric Mössbauer spectrometer SM-2201 developed on the basis of patents by Irkaev et al. (1987, 1990) and Vahonin et al. (1988a, 1988b). The noise of velocity signal of spectrometer was 1.5×10^{-3} mm/s, the drift of zero velocity point was $\pm 2.6 \times 10^{-3}$ mm/s, the nonlinearity of velocity signal was 0.01%, the systematic error of velocity

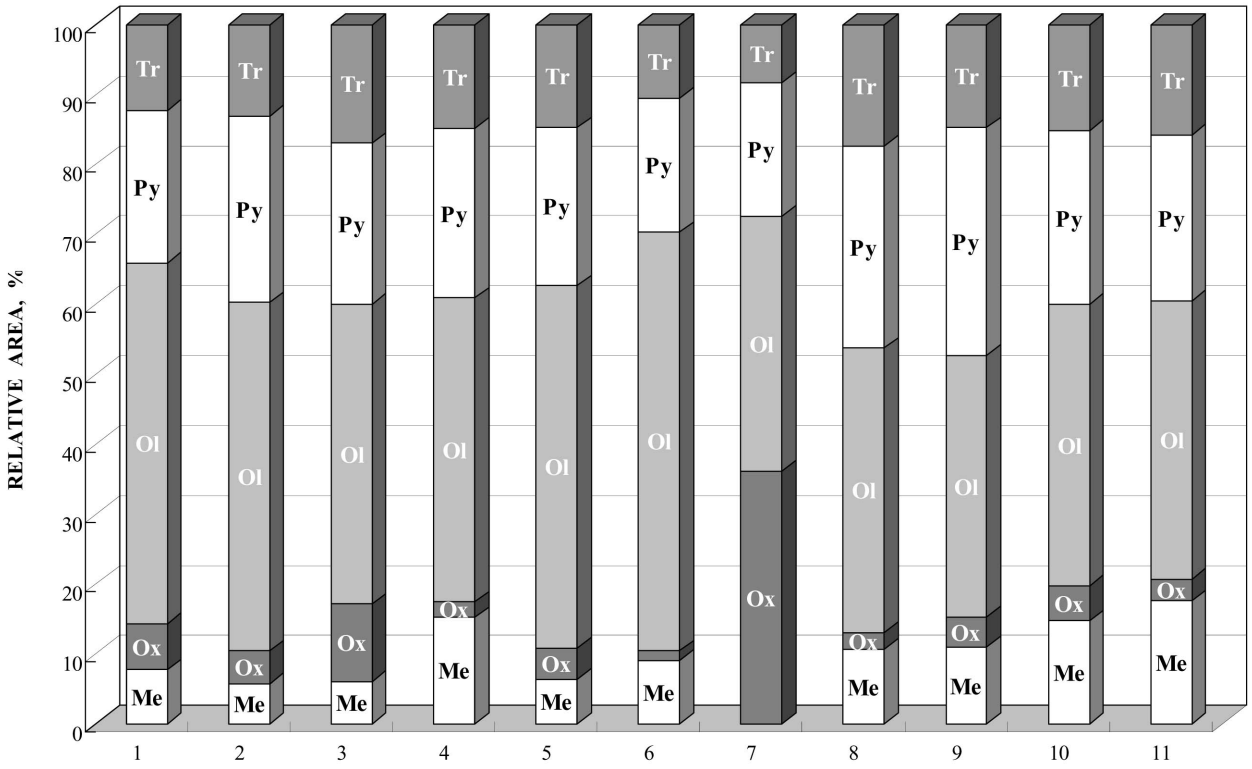

Fig. 3. Relative areas of components in Mössbauer spectra of ordinary chondrites. 1 = Saratov L4, 2 = Mount Tazerzait L5, 3 = Tsarev L5, 4 = Farmington L5, 5 = Mbale L5/6, 6 = Kunashak L6, 7 = Zubkovsky L6, 8 = Ochansk H4, 9 = Richardton H5, 10 = Vengerovo H5, 11 = Zvonkov H6) at room temperature. Me = metal, Ox = oxidized iron, Ol = olivine, Py = pyroxene and Tr = troilite.

setting was 0.025%, the temperature drift of velocity signal was 2×10^{-3} (mm/s)/°C. The 2.5×10^9 Bq ^{57}Co(Cr) source was used at room temperature. Mössbauer spectra were measured in transmission geometry with a moving absorber. This geometry excludes parabolic distortion of the spectrum and contribution of the ^{57}Fe in the beryllium window of the scintillator detector to the measured spectrum (Semionkin et al. 2005). These negative effects appear in the case of a moving source during spectra measurement with high statistics for samples with low total iron content or with low iron content in at least one compound in a mixture. Moreover, the source-detector distance can be minimal in geometry with moving absorber that leads to substantial increase of capacity during γ-ray registration and accelerates spectra measurement. Mössbauer spectra were measured with registration in 4096 channels with further presentation in 1024 channels by consequent summation of four neighbor channels. The signal/noise ratio for the lowest intensity peak in these spectra was ≥5 following the Romanovsky criterion to obtain statistically reliable data during further spectra fitting (Semionkin et al. 2005). Therefore, Mössbauer spectra were measured from 4 up to 20 days with statistics from 5.3 $\times 10^6$ to 28.3 $\times 10^6$ counts per channel for chondrites and ~12.5 $\times 10^6$ counts/channel for extracted metal. Mössbauer spectra were computer fitted with the least squares procedure using Lorentzian line shape. Line widths and intensities were equal for each line in doublet, line widths were equal for each line in sextet (except spectrum of metal extracted from Tsarev L5) and areas of sextet lines were fixed within the ratio S_{16}:S_{25}:S_{34} = 3:2:1. Mössbauer parameters isomer shift (δ), quadrupole splitting (ΔE_Q), magnetic hyperfine field (H_{eff}), line width (Γ) and subspectrum relative area (S) were determined. Experimental error for determination of the each spectra point was ±0.5 channel, errors for hyperfine parameters evaluation were ±1 channel while error for Γ evaluation was ±2 channels. It should be noted that spectrometer characteristics determined an integral velocity error which was several times lower than a half of channel value in mm/s during spectra measurements using 4096 channels. Criteria of the best fit were χ^2 values and physical meaning of parameters. The values of isomer shift are given relative to α-Fe at 295 K.

RESULTS AND DISCUSSION

Mössbauer Spectra

Mössbauer spectra of ordinary chondrites are shown in Fig. 1 (chemical group L) and Fig. 2 (chemical group H). These spectra are usual chondrite spectra consisting of

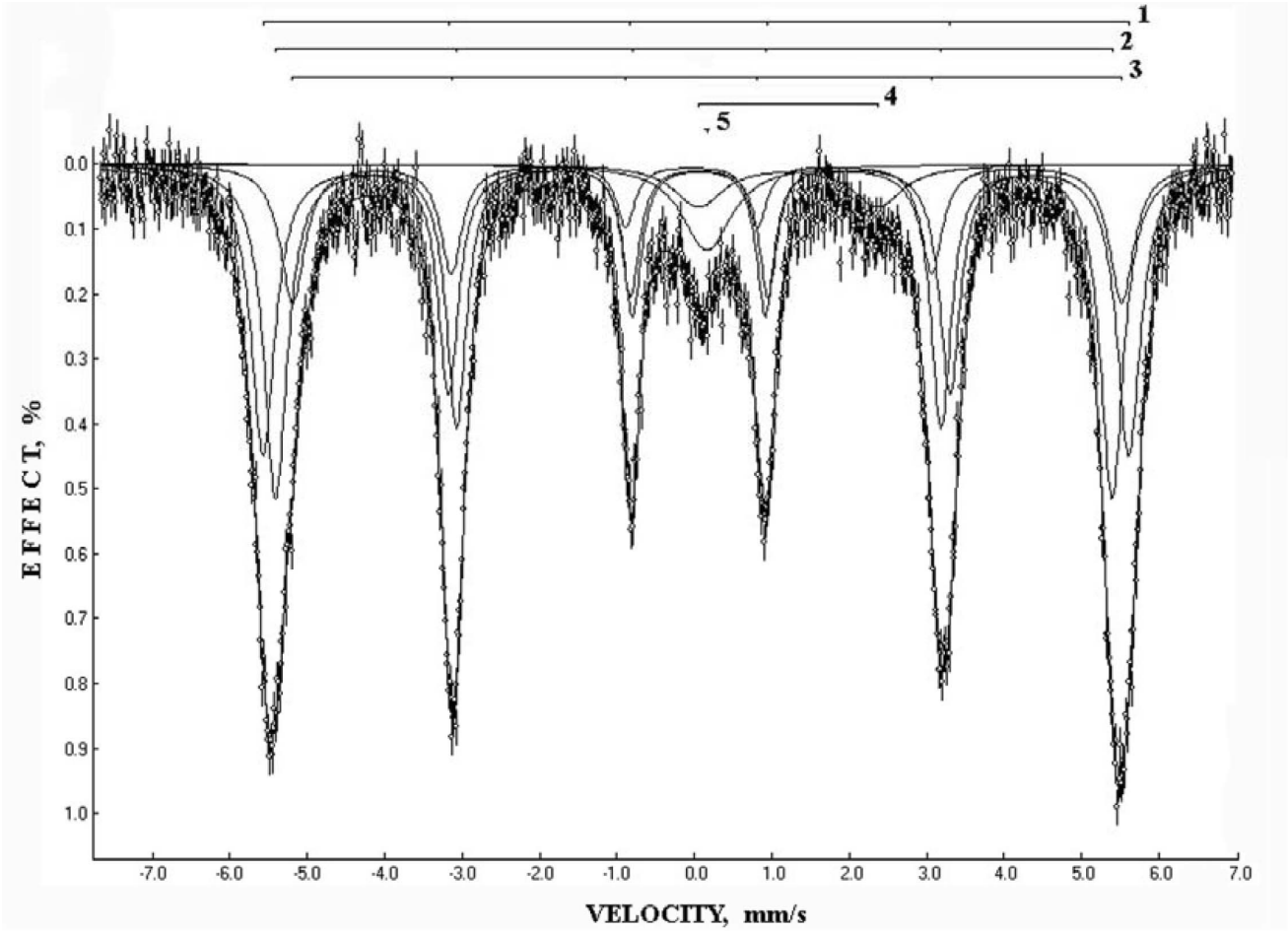

Fig. 4. Mössbauer spectrum of metal grains extracted from Tsarev L5. Components are given in Table 2. T = 295 K.

Table 2. Parameters of Mössbauer spectra of metal extracted from Tsarev L5.

Sample	Γ (mm/s)	δ (mm/s)	ΔE_Q (mm/s)	H_{eff} (kOe)	S (%)	Compound[a]
Metal extracted from Tsarev L5	0.372 ± 0.029	0.042 ± 0.014	–0.043 ± 0.014	347.2 ± 0.5	34.35	Fe(Ni, Co) (1)
	0.360 ± 0.029	0.027 ± 0.014	–0.066 ± 0.014	335.4 ± 0.5	38.21	Fe(Ni, Co) (2)
	0.386 ± 0.029	0.066 ± 0.014	0.202 ± 0.014	332.5 ± 0.5	16.97	Fe(Ni, Co) (3)
	0.776[b] ± 0.029	1.209 ± 0.014	2.311 ± 0.014	–	5.16	Residual silicates (4)
	0.776[b] ± 0.029	0.163 ± 0.014	–	–	5.31	Fe(Ni, Co) (5)

[a]Numbers of components in Fig. 4 are given in parenthesis.
[b]Parameters on the limit of variation.

components related to iron-bearing phases (metal, troilite, olivine, pyroxene, and oxidized iron) with different content. The spectrum of Zubkovsky L6 demonstrates the absence of metal and high level of oxidation. These spectra were fitted using one or two sextets to fit metal subspectra, one sextet to fit troilite subspectra, two quadrupole doublets to fit each subspectrum of olivine and pyroxene, and one quadrupole doublet to fit oxidized iron (Fe^{3+}). In the case of the Zubkovsky L6, the Mössbauer spectrum was fitted using two sextets to fit troilite subspectra, two quadrupole doublets to fit each subspectrum of olivine and pyroxene, and one quadrupole doublet and one sextet to fit oxidized iron. The results of the best fit are given in Table 1. It is well known that exact relation of S in complicated spectrum to iron content in correspondent species is possible in the case of the same Mössbauer effect probability in these species only (for instance, at low temperatures). Nevertheless, we can compare results obtained at room temperature for rough modal analysis. The differences of iron-bearing minerals content in ordinary chondrites are clearly seen in Fig. 3 on the basis of relative areas of its subspectra.

Mössbauer spectrum of metal grains extracted from Tsarev L5 is shown in Fig. 4. This spectrum is asymmetrical sextet with minor paramagnetic components. The best

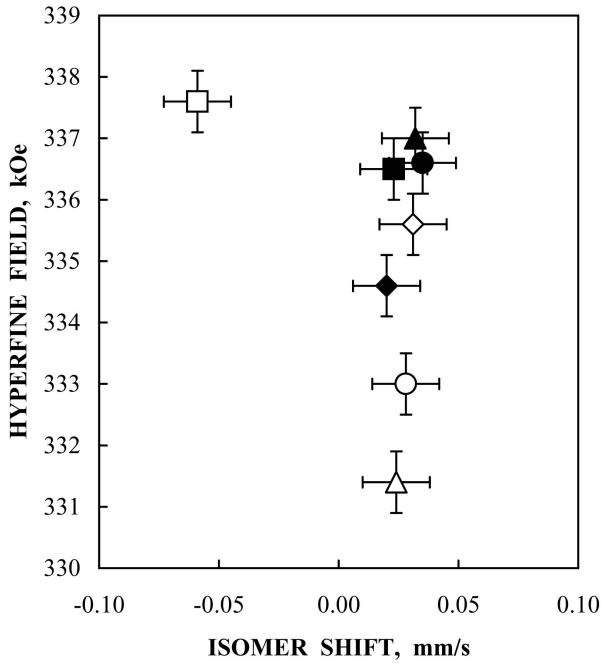

Fig. 5. Plot of Mössbauer hyperfine parameters for metal subspectra in ordinary chondrites which may be related to α-Fe(Ni, Co) mainly: ◇ = Saratov L4, ○ = Tsarev L5, □ = Farmington L5, △ = Mbale L5/6, ◆ = Ochansk H4, ● = Richardton H5, ■ = Vengerovo H5, ▲ = Zvonkov H6. T = 295 K.

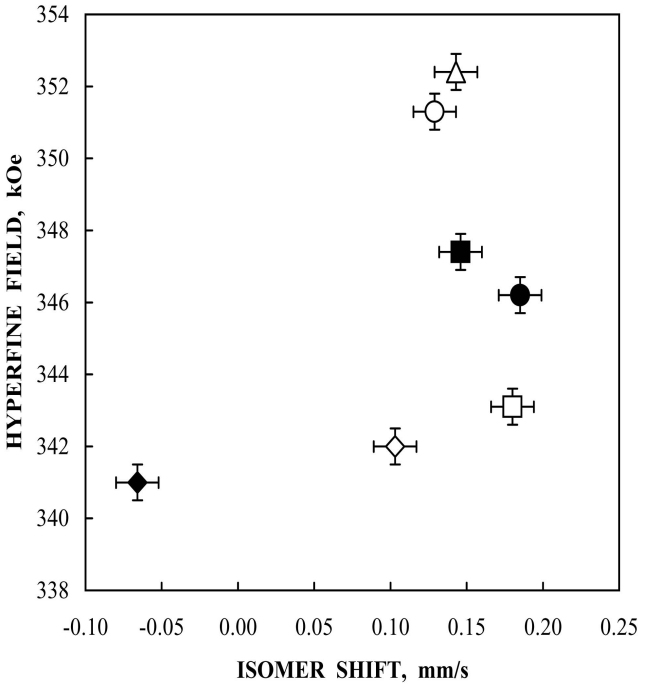

Fig. 6. Plot of Mössbauer hyperfine parameters for metal subspectra in ordinary chondrites which may be related to α′-Fe(Ni, Co) or α_2-Fe(Ni, Co): ◇ = Mount Tazerzait L5, ■ = Mount Tazerzait L5, ○ = Tsarev L5, □ = Farmington L5, △ = Mbale L5/6, ◆ = Kunashak L6, ● = Kunashak L6. T = 295 K.

spectrum fitting permitted us to reveal several different components: three magnetic sextets, one quadrupole doublet, and one paramagnetic singlet whose parameters are given in Table 2.

Metal

Metal subspectra of ordinary chondrite Mössbauer spectra were fitted using one or two magnetic sextets. This spectral component was initially fitted using one sextet for Mössbauer spectra of all ordinary chondrites. The values of Γ for the first and the sixth lines in sextets appeared to be different. In the case of chondrites Saratov L4, Ochansk H4, Richardton H5, Vengerovo H5, and Zvonkov H6, the values of Γ were in the range of ~0.41–0.49 mm/s. In contrast, in the case of chondrites Tsarev L5, Mount Tazerzait L5, Farmington L5, Mbale L5/6, and Kunashak L6 the values of Γ were in the range of ~0.52–0.58 mm/s. The broader lines were related to the presence of at least one additional sextet. It was supposed that if the values of Γ for the first and the sixth lines of one sextet used for metal component fitting exceeded 0.50 mm/s the superposition of at least two sextets should be used to fit this component. Thus, Mössbauer spectra of Saratov L4, Ochansk H4, Richardton H5, Vengerovo H5, and Zvonkov H6 were better fitted using one magnetic sextet while spectra of Tsarev L5, Mount Tazerzait L5, Farmington L5, Mbale L5/6, and Kunashak L6 were better fitted using two magnetic sextets (in this case χ^2 was slightly decreased). The values of H_{eff} for these sextets may be divided between the regions of 331–338 kOe and 340–353 kOe which are shown in the plots of hyperfine parameters (see Figs. 5 and 6). The first region of hyperfine fields was mainly related to α-Fe(Ni, Co) phase with different concentration of Ni and Co, while the second one was related to α′-Fe(Ni, Co) or α^2-Fe(Ni, Co) phases with different concentration of Ni and Co. It should be noted that the values of H_{eff} for the secondary kamacite α′-Fe(Ni, Co) with low Ni concentration (down to ~7 wt%) can be similar to those of α-Fe(Ni, Co) with upper Ni concentration.

Microphotographs of studied ordinary chondrites metal grains (except Ochansk H4 and Zubkovsky L6) in the polished section after etching with 2% HNO_3 solution in alcohol are shown in Fig. 7. The main metal phase in chondrites Saratov L4, Richardton H5, Vengerovo H5, Zvonkov H6 (Figs. 7a, and 7g–i, respectively) was kamacite α-Fe(Ni, Co). Very low content of taenite γ-Fe(Ni, Co) was found in chondrites Vengerovo H5 and Zvonkov H6. These data were in agreement with the results of Mössbauer spectra approximation using one sextet for metal. The values of H_{eff} for metal in these chondrites corresponded to kamacite α-Fe(Ni, Co). Microphotographs of Mount Tazerzait L5, Tsarev L5, Farmington L5, Mbale L5/6, and Kunashak L6 (Figs. 7b–f, respectively) demonstrated the presence of several phases in comparable quantities. For instance, metal of

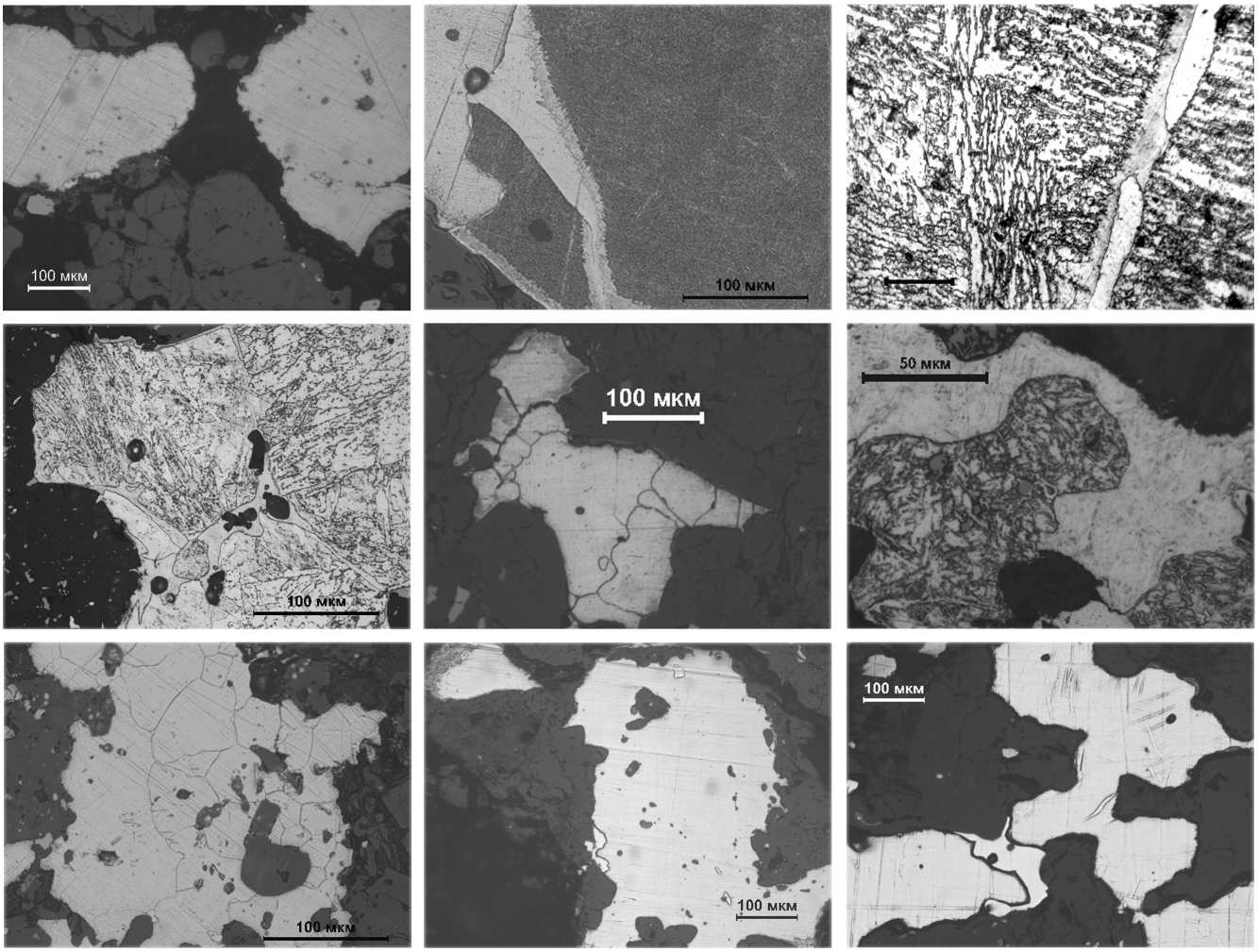

Fig. 7. Digital photomicrographs of metal grains in ordinary chondrites. Saratov L4 (a), Mount Tazerzait L5 (b), Tsarev L5 (c), Farmington L5 (d), Mbale L5/L6 (e), Kunashak L6 (f), Richardton H5 (g), Vengerovo H5 (h), Zvonkov H6 (i). 1 = kamacite α-Fe(Ni, Co); 2 = α_2-Fe(Ni, Co); 3 = secondary kamacite α′-Fe(Ni, Co); 4 = taenite γ-Fe(Ni, Co); 5 = plessite α′-Fe(Ni, Co) + γ-Fe(Ni, Co).

Farmington L5 consisted of plessite α′-Fe(Ni, Co) + γ-Fe(Ni, Co) and α_2-Fe(Ni, Co) phase. We supposed that value of H_{eff} = 337.6 kOe could be related to α′-Fe(Ni, Co) while value of H_{eff} = 343.1 kOe could be related to α_2-Fe(Ni, Co) phase. In the case of chondrite Mbale L5/6 metal consisted of kamacite α-Fe(Ni, Co) and α_2-Fe(Ni, Co) phase. Corresponding values of H_{eff} were 331.4 and 352.4 kOe, respectively. Chondrite Kunashak L6 contained metal consisting of kamacite α-Fe(Ni, Co) and plessite α′-Fe(Ni, Co) + γ-Fe(Ni, Co). We supposed that values of H_{eff} of 341.0 and 346.2 kOe might be related to kamacite α-Fe(Ni, Co) with higher Co concentration and α′-Fe(Ni, Co). On the other hand, metal of Mount Tazerzait L5 consisted of kamacite α-Fe(Ni, Co), α_2-Fe(Ni, Co), and plessite α′-Fe(Ni, Co) + γ-Fe(Ni, Co). In this case, two magnetic sextets were better fit of α-Fe(Ni, Co), α_2-Fe(Ni, Co), and α′-Fe(Ni, Co) contribution to the metal subspectrum. Metal of Tsarev L5 consisted of the same phases and their contribution was a better fit using two sextets. Differences of H_{eff} values could reflect different metal compositions of Mount Tazerzait L5 and Tsarev L5. Therefore, the Mössbauer study of extracted metal from Tsarev L5 was made (amount of other chondrites was not enough for metal extraction).

The best fitting of the Mössbauer spectrum of metal grains extracted from meteorite Tsarev L5 (Fig. 4) permitted us to reveal several different components: three sextets, one doublet and one singlet parameters of which are given in Table 2. The doublet corresponded to residual silicates in extracted metal (~5.2%), sextets corresponded to ferromagnetic phases in metal with different values of the effective magnetic field on the ^{57}Fe nucleus and singlet corresponded to paramagnetic phase in metal. Metallographic data of chondrite Tsarev L5 demonstrated that its matter was strong shock affected in the space (Migdisova et al. 1982; Leroux et al. 2000). Microphotograph of typical metal grain is shown in Fig. 7d.

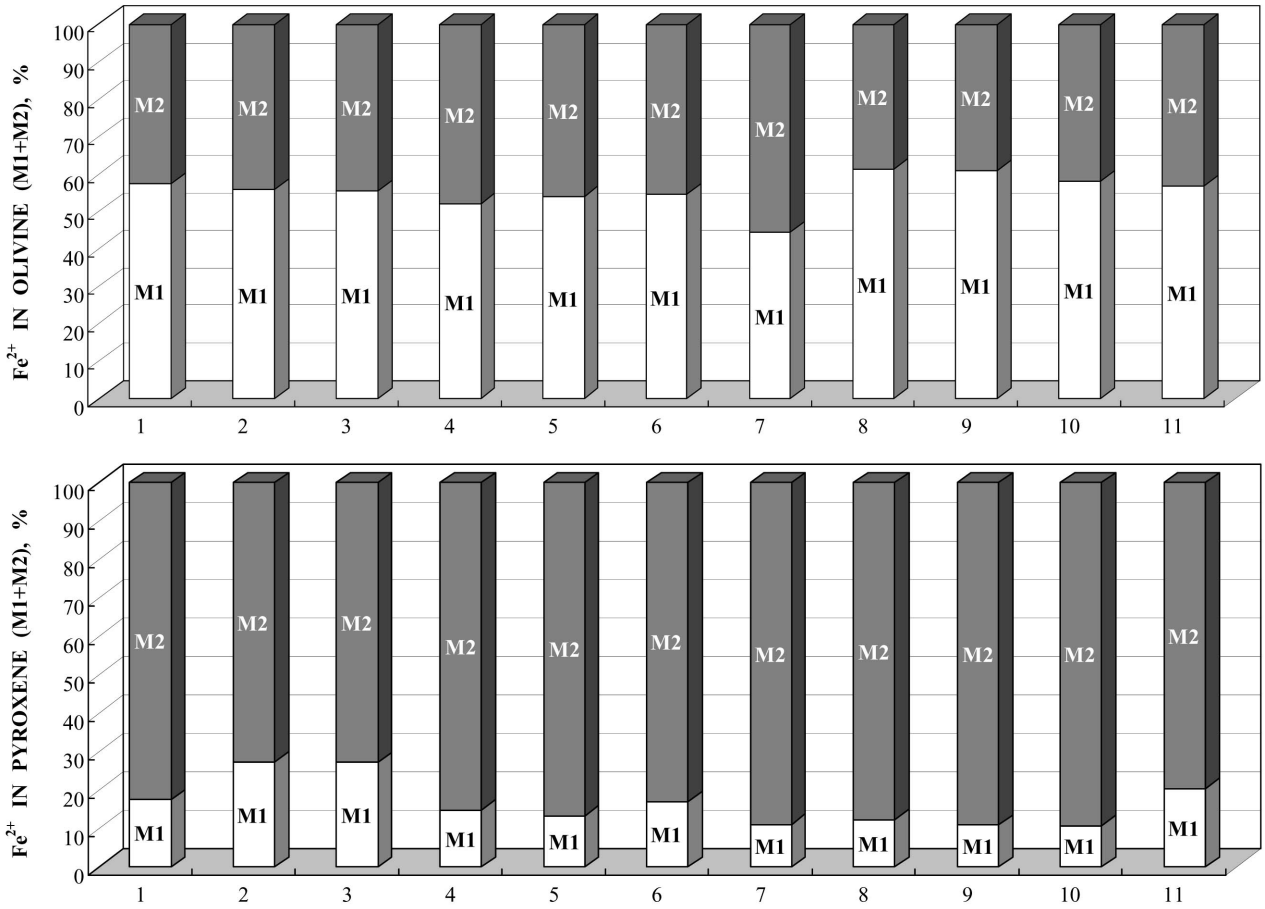

Fig. 8. Distribution of Fe^{2+} between M1 and M2 sites in olivine and pyroxene in ordinary chondrites (1 = Saratov L4, 2 = Mount Tazerzait L5, 3 = Tsarev L5, 4 = Farmington L5, 5 = Mbale L5/6, 6 = Kunashak L6, 7 = Zubkovsky L6, 8 = Ochansk H4, 9 = Richardton H5, 10 = Vengerovo H5, 11 = Zvonkov H6) on the basis of the room temperature Mössbauer spectra.

Electron microprobe analysis and metallography revealed the main metal phases in the grain such as: kamacite α-Fe(Ni, Co) with Ni concentration of ~7.4 wt% (at the border of metal grains and silicates); non-equilibrium α_2-Fe(Ni, Co) phase with high Ni concentration of up to 20%; secondary kamacite α′-Fe(Ni, Co) with Ni concentration of ~10 wt% that appeared as a result of α_2-Fe(Ni, Co) phase decomposition with precipitation of taenite (γ-Fe(Ni, Co) phase with high Ni concentration); and plessite structure α′-Fe(Ni, Co) + γ-Fe(Ni, Co). The taenite phase was presented in plessite in the form of particles smaller than 1 μm and was not well resolved using optical microscope. Increasing of the effective magnetic field value on the ^{57}Fe nucleus for Fe(Ni, Co) alloys was observed with increasing Ni concentration from 0 to ~25 wt% (Vincze et al. 1974; Oshtrakh et al. 2004; Grokhovsky et al. 2005a). Therefore, the sextet 3 (H_{eff} = 332,5 kOe) was related to kamacite α-Fe(Ni, Co), the sextet 2 (H_{eff} = 335.4 kOe) was related to secondary kamacite α′-Fe(Ni, Co) in plessite and the sextet 1 (H_{eff} = 347.2 kOe) was related to α_2-Fe(Ni, Co) phase. The singlet 5 was related to paramagnetic taenite γ-Fe(Ni, Co) in plessite. It was interesting to point that these results were similar to the data from Ludwig et al. (2001) for the Mössbauer study of extracted metal from El Hammami H5 where the authors distinguished four ferromagnetic components with H_{eff} varied from ~324 to ~350 kOe related to α-Fe(Ni). However, the authors related these components to kamacites only, but this seems to be spurious. Earlier, Kong et al. (1995) observed sextet with H_{eff} about 340 kOe related to α-Fe(Ni) and two sextets with H_{eff} about 321 and 290 kOe related to disordered and ordered γ-Fe(Ni), respectively, in Mössbauer spectra of metal extracted from Richardton H5 and treated by HF for different time.

Olivine and Pyroxene

The fit of the olivine component using two quadrupole split doublets demonstrated similar results for all Mössbauer spectra of meteorites. In accordance with the results of Morozov et al. (2005a, 2005b), quadrupole doublet with higher relative area was related to M1 site and the other doublet was related to M2 sites. Distributions of Fe^{2+} ions between M1 and M2 sites in olivine obtained on the basis of

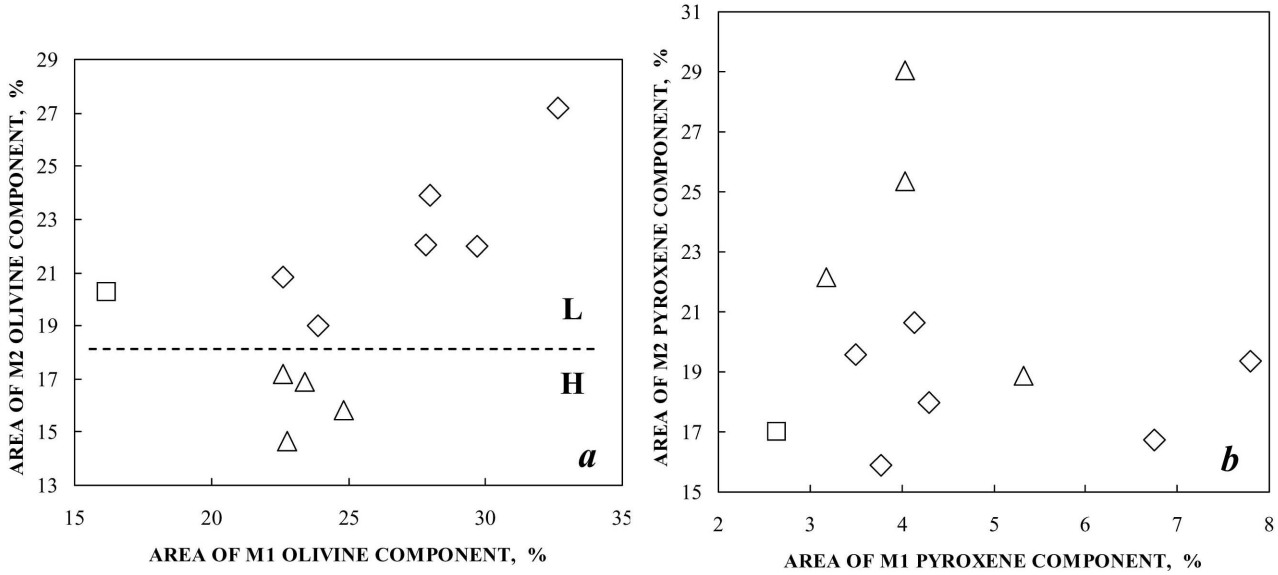

Fig. 9. Plots of relative areas of Mössbauer subspectra related to M1 and M2 sites in olivine (a) and pyroxene (b) for ordinary chondrites: ◇ = L chondrites (Saratov L4, Mount Tazerzait L5, Tsarev L5, Farmington L5, Mbale L5/6, Kunashak L6), □ = high oxidized L chondrite (Zubkovsky L6), △ = H chondrites (Ochansk H4, Richardton H5, Vengerovo H5, Zvonkov H6).

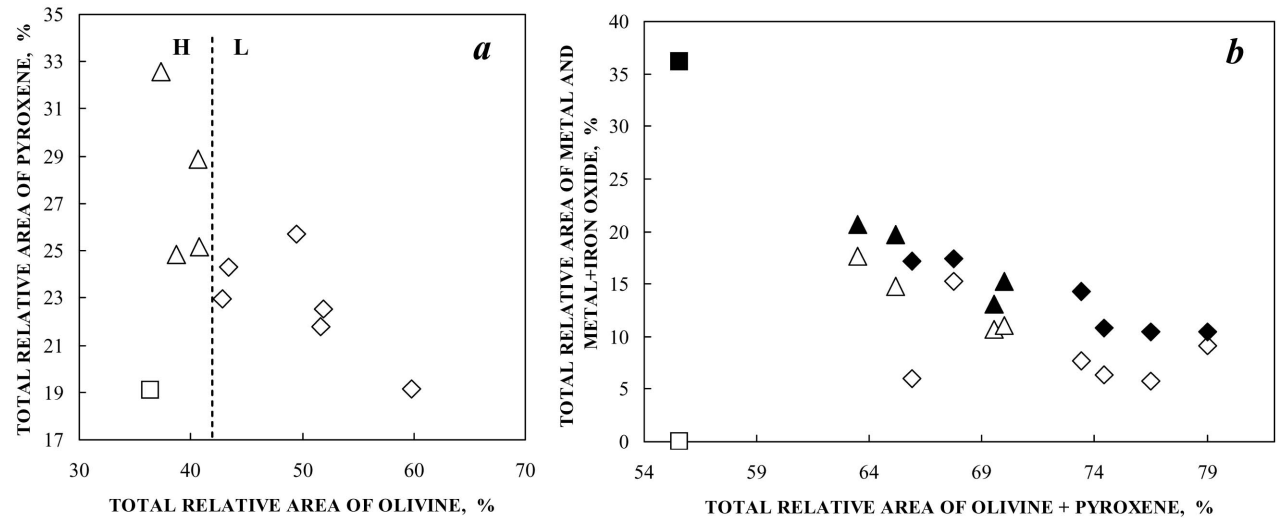

Fig. 10. Plots of total relative areas of Mössbauer subspectra of olivine and pyroxene (a) and metal (metal + oxidized iron) and olivine + pyroxene (b) for ordinary chondrites: ◇ = L chondrites (Saratov L4, Mount Tazerzait L5, Tsarev L5, Farmington L5, Mbale L5/6, Kunashak L6), □ = high oxidized L chondrite (Zubkovsky L6), △ = H chondrites (Ochansk H4, Richardton H5, Vengerovo H5, Zvonkov H6). Black symbols (b) indicate the case of total relative areas of metal + oxidized iron.

relative areas of olivine components in Mössbauer spectra of chondrites are shown in Fig. 8a. Olivine M1 sites in studied chondrites except Zubkovsky L6 contained from ~52 to ~61%, while olivine M2 sites contained from ~48 to ~39% of total Fe^{2+} ions. In the case of Zubkovsky L6, olivine M1 sites contained ~44%, while M2 sites contained ~56% of total Fe^{2+} ions. Similar results for studied chondrites were obtained during the fit of the pyroxene component using two quadrupole split doublets too. On the basis of Pasternak et al. (1992), Van Alboom et al. (1993), and Wang et al. (2005) data, quadrupole doublet with lower relative area was related to M1 site and the other doublet was related to M2 sites. Distributions of Fe^{2+} ions between M1 and M2 sites in pyroxenes on the basis of relative areas of pyroxene components in Mössbauer spectra are shown in Fig. 8b. Pyroxene M1 sites in studied ordinary chondrites contained from ~11 to ~27% while M2 sites contained from ~89 to ~73% of total Fe^{2+} ions. This data was in agreement with previous Mössbauer studies of pure synthetic and natural olivines and pyroxenes.

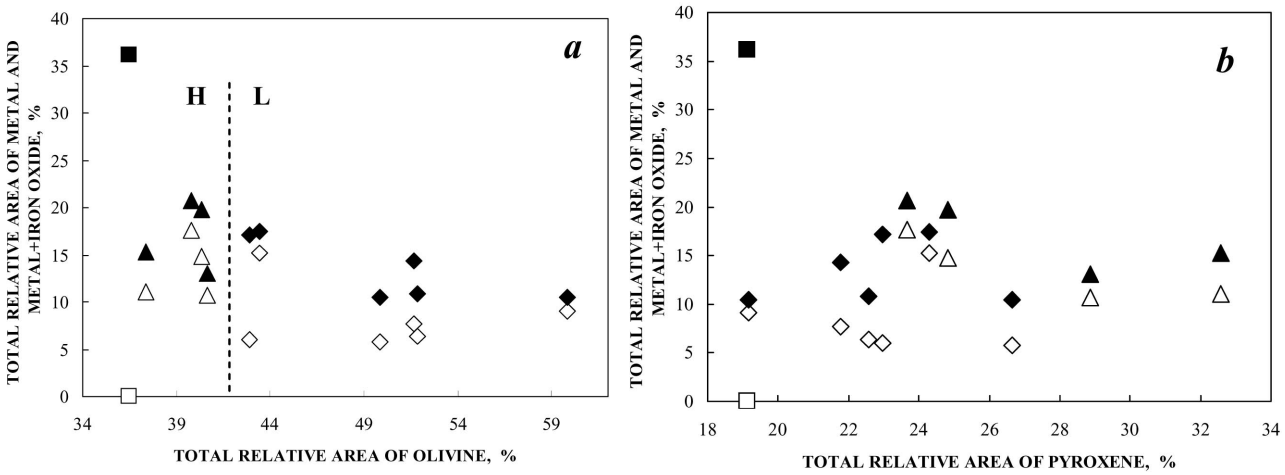

Fig. 11. Plots of total relative areas of Mössbauer subspectra of metal (metal + oxidized iron) and olivine (a) or pyroxene (b) for ordinary chondrites: ◇, ◆ = L chondrites (Saratov L4, Mount Tazerzait L5, Tsarev L5, Farmington L5, Mbale L5/6, Kunashak L6), □, ■ = high oxidized L chondrite (Zubkovsky L6), △, ▲ = H chondrites (Ochansk H4, Richardton H5, Vengerovo H5, Zvonkov H6). Open symbols indicate the case of total relative areas of metal, while black symbols indicate the case of total relative areas of metal + oxidized iron.

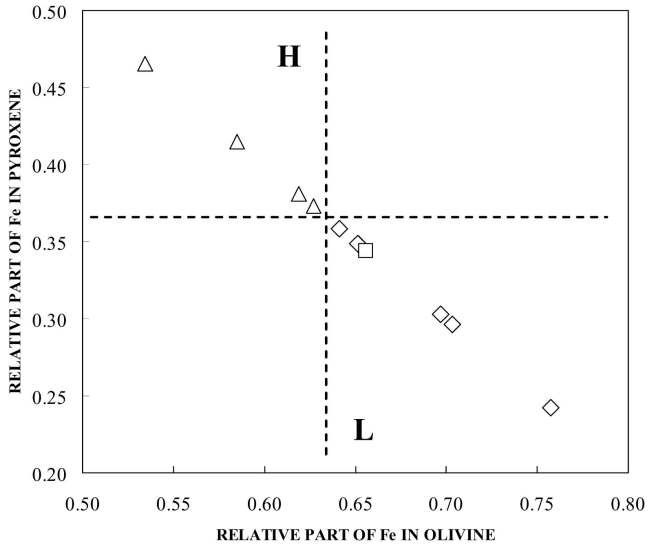

Fig. 12. Plot of relative parts of Fe in silicates on the base of relative areas of Mössbauer subspectra of olivine and pyroxene in ordinary chondrites: ◇ = L chondrites (Saratov L4, Mount Tazerzait L5, Tsarev L5, Farmington L5, Mbale L5/6, Kunashak L6), □ = high oxidized L chondrite (Zubkovsky L6), △ = H chondrites (Ochansk H4, Richardton H5, Vengerovo H5, Zvonkov H6).

Comparison of the plots of relative areas of Mössbauer subspectra of M1 and M2 sites in both olivine and pyroxene is shown in Fig. 9. It was interesting to observe some differences for olivine in L and H chondrites except Zubkovsky L6 (Fig. 9a). Relative areas of M2 sites in olivine were higher than ~18.5% for L chondrites. In contrast, there were no similar differences for relative areas of M1 and M2 sites in pyroxene. Earlier, Verma et al. (2003) proposed some systematic of H, L, and LL chondrites on the basis of relative areas of Mössbauer spectra components. In Fig. 10a the plot of total relative areas of olivine and pyroxene demonstrates some differences in the regions of H and L chondrites. This fact is similar to the data by Verma et al. (2003); however, to distinguish H and L chondrites total relative areas of olivine are more acceptable. In this case, we can suppose that the total relative area of olivine in Mössbauer spectra of L chondrites should not be lower than ~42%, while that in Mössbauer spectra of H chondrites should not exceed ~42%. On the other hand, the plot of total relative areas of metal (metal + oxidized iron) versus olivine + pyroxene (Fig. 10b) did not allow us to observe a clear distinction between H and L chondrites in comparison with the data of Verma et al. (2003). It should be noted that in the case of low chondrite weathering, the total relative area of metal and oxidized iron subspectra can be considered as rough estimation of the initial metal in chondrite (the Mössbauer effect probability is not the same for metal and oxidized iron at room temperature). Distinguishing of H and L chondrites was also possible in the plots of the total relative areas of metal (metal + oxidized iron) subspectra versus olivine subspectra (Fig. 11a), in contrast to pyroxene subspectra (Fig. 11b). The case of the plot with total olivine areas (Fig. 11a) also demonstrated that total relative area of olivine in Mössbauer spectra of L chondrites should not be lower than ~42%, while that in Mössbauer spectra of H chondrites should not exceed ~42%, as in the case of the plot in Fig. 9a. It is possible that the Mössbauer effect probability for ^{57}Fe in olivine and pyroxene is similar. Therefore, we can determine relative parts of Fe in silicate phases. The differences between L and H chondrites are clearly seen in the plot of relative parts of Fe in olivine and pyroxene (Fig. 12).

Analysis of Mössbauer hyperfine parameters for M1

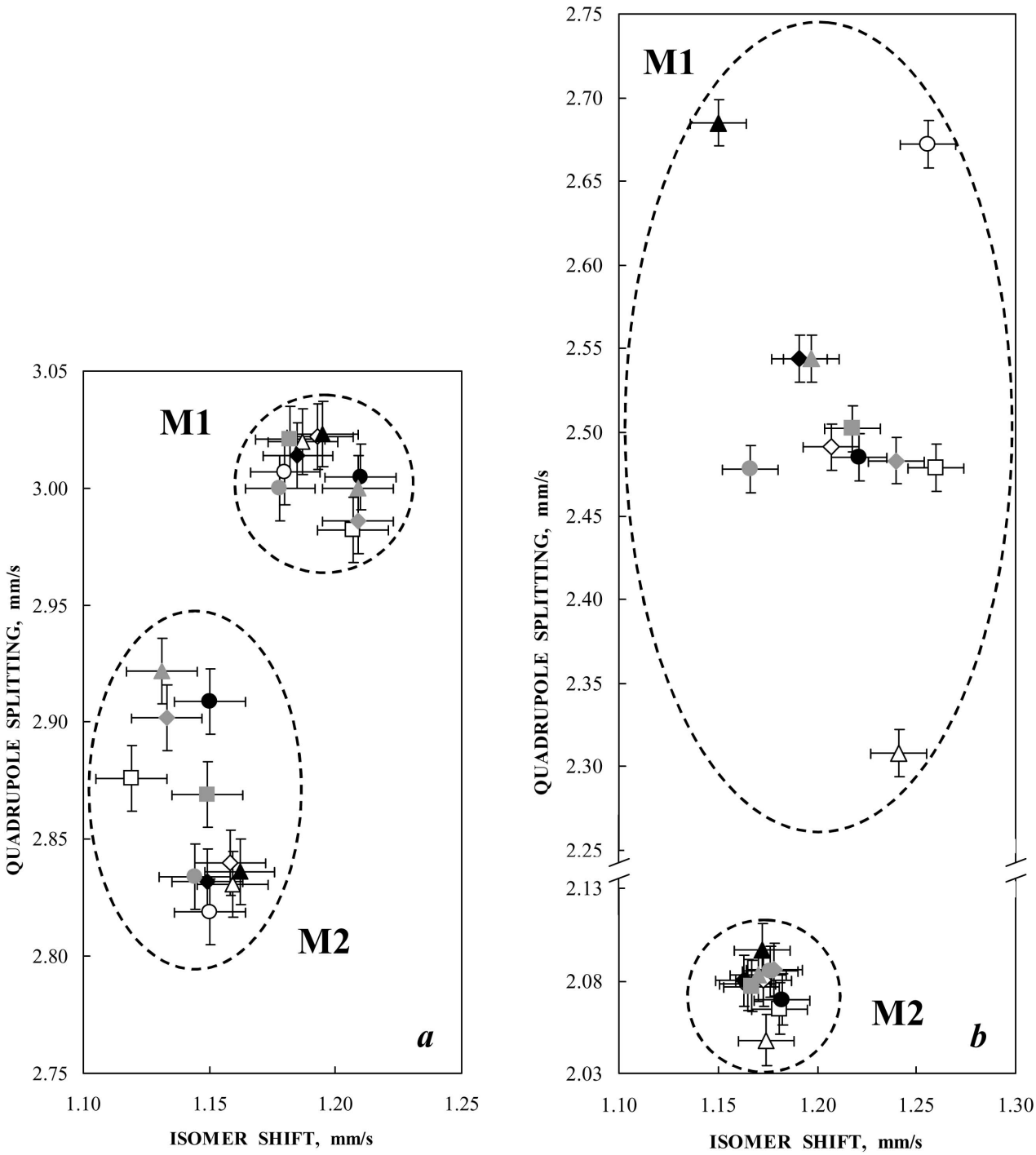

Fig. 13. Plots of Mössbauer hyperfine parameters for M1 and M2 sites in olivine (a) and pyroxene (b) in ordinary chondrites: ◇ = Saratov L4, □ = Mount Tazerzait L5, △ = Tsarev L5, ○ = Farmington L5, ◆ = Mbale L5/6, ● = Kunashak L6, ▲ = Zubkovsky L6, ■ = Ochansk H4, ◆ = Richardton H5, ▲ = Vengerovo H5, ● = Zvonkov H6. T = 295 K.

and M2 sites in olivine and pyroxene in ordinary chondrites demonstrated several differences. The plots of quadrupole splitting versus isomer shift for M1 and M2 sites are shown in Fig. 13. The values of hyperfine parameters for olivine M1 sites appeared to be close and varied in the range of about 4.5 experimental errors. In contrast, the values of hyperfine parameters for olivine M2 sites varied in a more extended range (two times larger for quadrupole splitting). These facts mean that Fe^{2+} ions in M1 sites of chondrite olivine have a similar environment with very small variation, while Fe^{2+} ions in M2 sites have slightly different stereochemistry reflected by a larger dispersion of hyperfine

Table 3. Calculated values of distribution coefficient and temperature of equilibrium cation distribution in pyroxene and olivine in selected chondrites.

Chondrite	X_{Fs} or X_{Fa}	X_{M1} (%)	X_{M2} (%)	r	K_D	T (K)
			Pyroxene			
Mbale L5/6	0.22	13.3	86.7	0.15	0.10	822
Farmington L5	0.21	14.9	85.1	0.18	0.12	884
Tsarev L5	0.20	27.2	72.8	0.37	0.30	1370
Zubkovsky L6	0.21	11.2	88.8	0.13	0.08	767
			Olivine			
Mbale L5/6	0.25	53.9	46.1	1.17	1.24	1192
Farmington L5	0.24	52.1	47.9	1.09	1.12	2265
Tsarev L5	0.24	55.7	44.3	1.26	1.35	834
Kunashak L6	0.23	54.6	45.4	1.20	1.27	1051
Saratov H4	0.24	57.5	42.5	1.35	1.48	638
Vengerovo H5	0.19	57.7	42.3	1.36	1.46	662
Zvonkov H6	0.19	56.8	43.2	1.32	1.40	745

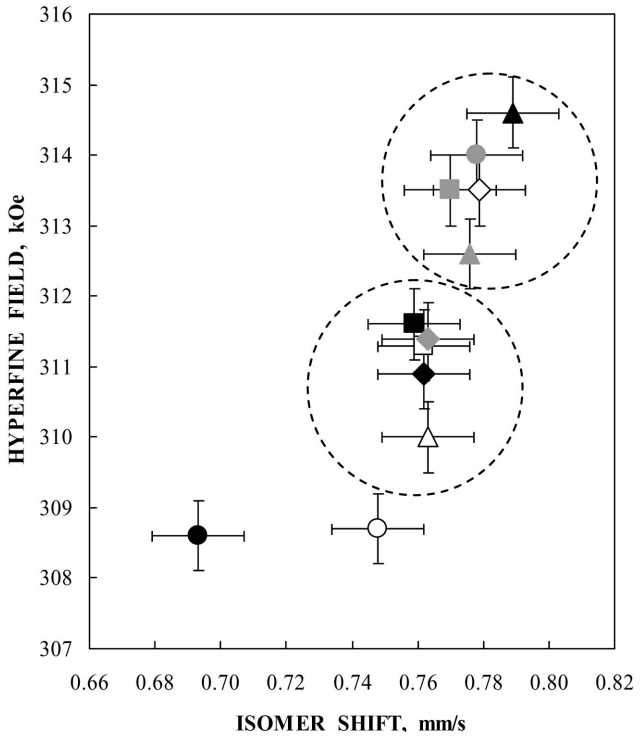

Fig. 14. Plot of Mössbauer hyperfine parameters for troilite in ordinary chondrites: ◇ = Saratov L4, □ = Mount Tazerzait L5, △ = Tsarev L5, ○ = Farmington L5, ◆ = Mbale L5/6, ■ = Kunashak L6, ▲ = Zubkovsky L6, ● = Zubkovsky L6, ◆ = Ochansk H4, ■ = Richardton H5, ▲ = Vengerovo H5, ● = Zvonkov H6. T = 295 K.

parameters. The higher value of ΔE_Q relates to a higher value of the electric field gradient that is a result of a higher level of crystal symmetry distortion. The data for pyroxene demonstrated an inverse figure. The values of hyperfine parameters for pyroxene M1 sites in chondrites varied in a wider range than those for olivine M2 sites. On the other hand, the values of hyperfine parameters for pyroxene M2 sites appeared to be close and varied in the same range as those for olivine M1 sites. These results reflected different stereochemistry of the Fe^{2+} environment in M1 sites of pyroxene while Fe^{2+} ions in M2 sites of pyroxene had a similar environment in chondrites.

It is well known that Fe^{2+} and Mg^{2+} distribution between M1 and M2 sites in olivines and pyroxenes is related to the temperature of equilibrium cation distribution and therefore to the thermal history of terrestrial and extraterrestrial minerals (see Malysheva 1975; Wang et al. 2005). A Fe^{2+}–Mg^{2+} distribution coefficient (K_D) between M1 and M2 sites in both olivines and pyroxenes can be defined as:

$$K_D = \frac{X_{Fe}^{M1} \cdot X_{Mg}^{M2}}{X_{Fe}^{M2} \cdot X_{Mg}^{M1}}, \quad (1)$$

where X_{Fe}^{M1} is the mole fraction of Fe^{2+} in the M1 sites, X_{Mg}^{M1} is the mole fraction of Mg^{2+} in the M1 sites, etc. If the Mössbauer effect probability is equal for ^{57}Fe in both M1 and M2 sites, then

$$\frac{X_{Fe}^{M1}}{X_{Fe}^{M2}} = \frac{S_{M1}}{S_{M2}} = r, \quad (2)$$

where S_{M1} and S_{M2} are relative areas of correspondent components in Mössbauer spectra. To determine the mole fraction of Mg^{2+} in M1 and M2 sites of olivine we can use Fa content, while in the case of pyroxene we can use ferrosilite (Fs) content:

$$X_{Mg}^{M1} = 1 - \frac{r \cdot Y_{Fe}}{1 + r} \quad (3)$$

and

$$X_{Mg}^{M2} = 1 - \frac{Y_{Fe}}{1 + r}, \quad (4)$$

where $Y_{Fe} = 2X_{Fs}$ for pyroxenes and $Y_{Fe} = 2X_{Fa}$ for olivines, X_{Fs} and X_{Fa} are molar fractions of Fe^{2+} (in unit portion) for pyroxenes and olivines, respectively. Then Equation 1 for K_D can be modified as:

$$K_D = \frac{r \cdot (r + 1 - 2X_{Fs})}{1 + r - 2r \cdot X_{Fs}} \quad (5)$$

and

$$K_D = \frac{r \cdot (r + 1 - 2X_{Fa})}{1 + r - 2r \cdot X_{Fa}}. \quad (6)$$

Thus, Equation 1 for K_D can be presented in the forms of Equations 5 and 6 that allow rough estimation of K_D on the basis of relative areas of M1 and M2 components of pyroxene and olivine Mössbauer subspectra as well as Fs and Fa data. Further, the equilibrium temperature can be obtained using its relation to K_D. For instance, Malysheva (1975) proposed this equation for olivines:

$$-\Delta G = R \cdot T \cdot \ln K_D, \quad (7)$$

where ΔG is the Gibbs energy (20935 J for olivine), R = 8.31 J/K mol. Using this equation values of T for olivine from several chondrites were determined (see Table 3). Wang et al. (2005) obtained this equation for pyroxenes.

$$\ln K_D = 0.391 - \frac{2205}{T}. \quad (8)$$

Calculated values of K_D and T for pyroxene and olivine in selected chondrites are given in Table 3. The calculated temperatures appeared to be reliable for chondrite pyroxenes. A higher temperature for pyroxene of Tsarev L5 may be a result of strong shock and reheating of this chondrite. Therefore, Fe^{2+} ions were redistributed in pyroxene of Tsarev L5 while equilibrium temperature for olivine was reliable. In the case of olivine an unusually high temperature obtained for Farmington L5 may also be related to strong shock and reheating. This indicates that determination of cation ordering temperature in the case of reheating events cannot be correct.

Troilite

Mössbauer parameters of troilite in all chondrite spectra except Zubkovsky L6 were similar to those of other chondrite studies (see, for instance, Forder et al. 2001; Verma et al. 2003). However, in the plot of the hyperfine parameters (Fig. 14) some differences of H_{eff} are clearly seen. Two regions marked with dashed lines contained two groups of chondrites which troilite subspectra had the same δ within the experimental error and slightly different H_{eff}. Subspectrum of troilite in Farmington L5 demonstrated the lowest value of H_{eff} in comparison with other chondrites and close to previous data for Farmington L5 (Forder et al. 2001). Differences of H_{eff} for troilite in these chondrites may be a result of small concentration or structural variations in FeS. In the case of Zubkovsky L6 subspectrum of troilite with asymmetrical first and sixth lines of sextet (Fig. 1g) was fitted using two sextets with different δ and H_{eff}. These parameters were different from possible parameters of iron oxides and hydroxides in the magnetic states. This result may be related to non-stoichiometry of FeS due to possible partial removal of Fe during the weathering process. Removal of Fe can be confirmed by the lowest total relative area of troilite in Mössbauer spectrum of Zubkovsky L6. Earlier several sextets were found in Mössbauer spectra of synthetic samples of $Fe_{1-x}S$ (Kruse 1990). It is possible that higher level of Zubkovsky L6 weathering may also affect the troilite content and structure (see also results of Skinner et al. 2004).

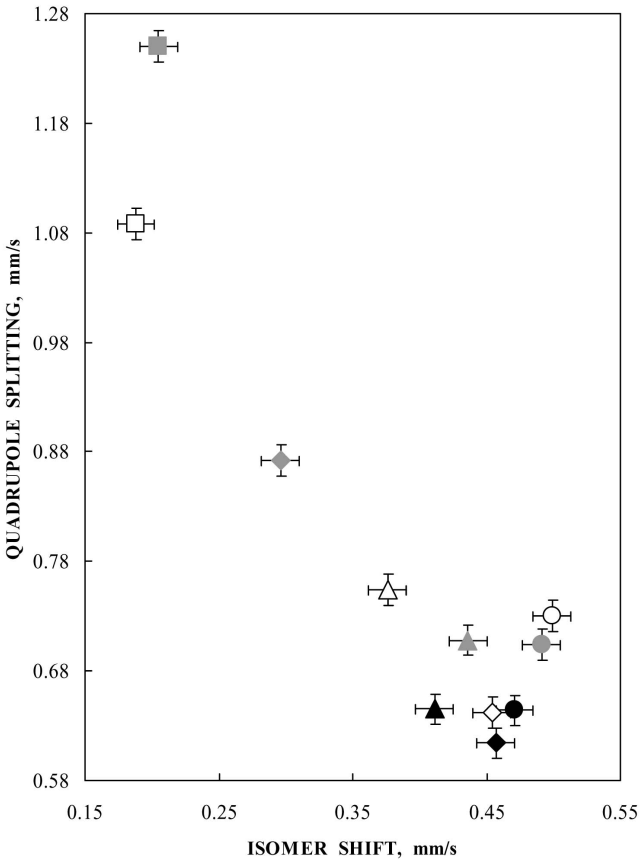

Fig. 15. Plot of Mössbauer hyperfine parameters for paramagnetic oxidized iron in ordinary chondrites: ◇ = Saratov L4, □ = Mount Tazerzait L5, △ = Tsarev L5, ○ = Farmington L5, ◆ = Mbale L5/6, ● = Kunashak L6, ▲ = Zubkovsky L6, ■ = Ochansk H4, ◆ = Richardton H5, ▲ = Vengerovo H5, ● = Zvonkov H6. T = 295 K.

Oxidized Iron

Mössbauer spectra of all studied chondrites demonstrated the presence of different quantities of Fe^{3+} compounds from ~1.4% to ~36.1%. Previously, in Mössbauer spectra of the same samples presented in 512 channels, Fe^{3+} compounds were found in part of chondrites (see Zhiganova et al. 2005). Samples of all chondrites except Zubkovsky L6 contained a paramagnetic ferric component only, while Zubkovsky L6 contained a ferric compound in paramagnetic and magnetic

states at room temperature. Moreover, this sample of Zubkovsky L6 contained no metal, the lowest amounts of troilite (total S was about 8%) and olivine (total S was about 36.5%), and an extremely large amount of Fe^{3+} compound (total S was about 36.1%). It is possible that all metal in this sample was oxidized as well as parts of Fe in troilite and olivine Fe^{2+} were oxidized. Bland et al. (1997) showed that oxidation of olivine Fe^{2+} during the weathering process was preferable after metal oxidation. Therefore, data for Zubkovsky L6 in the plots with relative areas of olivine and oxidized iron were unusual for L chondrites and marked with another symbol. The distribution of Fe^{2+} between M1 and M2 sites in olivine shown in Fig. 8 demonstrated differences for Zubkovsky L6: Fe^{2+} content in M2 sites was about 10% higher than that in other chondrites. In this case, we can suppose that Fe^{2+} in M1 sites of olivine oxidized easier than in M2 sites.

Mössbauer hyperfine parameters of paramagnetic Fe^{3+} compounds found in ordinary chondrites appeared to be different (see the plot in Fig. 15), however, these values were corresponding to the regions of ΔE_Q and δ for the high spin ferric iron. These results except Mount Tazerzait L5 and Ochansk H4 were in agreement with data of Bland et al. (1996, 1998b), where some variations of ΔE_Q and δ were found. Mössbauer parameters of these Fe^{3+} compounds may be related to ferric hydrous oxides, preferably akaganeite (β-FeOOH). It is well known that Néel temperatures for ferric hydrous oxides varied in a wide temperature region: about 400 K for α-FeOOH, about 295 K for β-FeOOH, about 440 K for δ-FeOOH and about 570 K for ε-FeOOH (Murad and Johnston 1987). Therefore, β-FeOOH with small particle sizes is the most appropriate compound that was in paramagnetic or superparamagnetic state at room temperature. Previous room temperature Mössbauer study of iron-dextran complexes containing β-FeOOH showed ΔE_Q values within the range of 0.68–0.74 mm/s and δ values within the range of 0.35–0.37 mm/s (Oshtrakh et al. 2001). However, Mössbauer study of iron meteorites weathering products (Grokhovsky et al. 2005a, 2005b) demonstrated higher values of δ for β-FeOOH (~0.41 mm/s). Earlier studies of subjects containing β-FeOOH showed that δ values varied from about 0.36 mm/s at room temperature to about 0.46 mm/s at liquid nitrogen temperature (Murad and Johnston [1987]; Oshtrakh et al. [2001]). Similar room temperature hyperfine parameters were observed for ferrihydrite and superparamagnetic α-FeOOH particles. Therefore, it is possible that weathering process in studied chondrites except Mount Tazerzait L5 and Ochansk H4 led to formation of ferric hydrous oxides such as β-FeOOH, ferrihydrite or ultra fine particles of α-FeOOH with various impurities (small ions) effecting the values of δ and ΔE_Q (see also Murad and Johnston 1987). To distinguish these ferric hydrous oxides low temperature Mössbauer measurements are required to observe temperatures of magnetic phase transition. In the case of Zubkovsky L6 with higher level of weathering, Mössbauer spectrum (Fig. 1g) demonstrated the presence of additional magnetic component, which may be a result of β-FeOOH particle formation and the beginning of magnetic phase transition. The values of δ and ΔE_Q for Mount Tazerzait L5 and Ochansk H4 were different from other chondrites and did not correspond to β-FeOOH or ferrihydrite. However, the value of ΔE_Q for aged ferric hydrolysis dimers $[(H_2O)_4Fe(OH)_2Fe(H_2O)_4]^{4+}$ with goethitic character was 1.20 mm/s at room temperature (Murad and Johnston 1987). Therefore, it is possible that the weathering products in Ochansk H4 and Mount Tazerzait L5 may be various ferric hydrolysis dimers or polymers. It should be noted that in an earlier Mössbauer study of weathered Antarctic chondrites the components of Fe^{3+} with δ~0.33–0.37 mm/s and ΔE_Q~1.23–1.32 mm/s were observed in some meteorites (Solberg and Burns 1989). In general, the formation of each weathering product depends on the weathering process and environmental conditions as well as terrestrial age of a chondrite. In this study, all chondrites except Zubkovsky L6 were falls with terrestrial ages up to 115 years. However, there was no correlation between terrestrial age and weathering grade in contrast to Bland et al. (1996, 1998b), where studied chondrites were in the same conditions. Therefore, the weathering processes in the chondrites studied depended on the conditions in which these samples were kept.

CONCLUSION

New measurement of 11 ordinary chondrites using a highly stable precision Mössbauer spectrometer with high-velocity resolution permitted us to obtain Mössbauer spectra with good quality to distinguish complicated spectra. Detailed analysis of Mössbauer parameters permitted us to reveal the presence of different Fe(Ni, Co) phases in metal and distinguish M1 and M2 sites in olivine and pyroxene of the bulk chondrites. Mössbauer study of extracted metal grains from Tsarev L5 revealed three magnetic α-Fe(Ni, Co), α′-Fe(Ni, Co), α_2-Fe(Ni, Co) phases and one paramagnetic γ-Fe(Ni, Co) phase. As for M1 and M2 sites in olivine and pyroxene, differences of Mössbauer hyperfine parameters were observed for ^{57}Fe in these sites in both olivine and pyroxene. It was shown that L and H chondrites were distinguished in the plot of relative areas of spectral components related to M1 and M2 sites in olivine. A rough estimation of cation equilibrium temperatures in olivine and pyroxene was made on the basis of relative areas of subspectra related to M1 and M2 sites in silicates. Differences of Mössbauer hyperfine parameters were also revealed for troilite and oxidized iron in various chondrites. These results demonstrated that Mössbauer spectra of ordinary chondrites measured with high-velocity resolution appeared to be more informative for further characterization of meteorites.

Acknowledgments—This work was supported in part by a grant from the Russian Foundation for Basic Research no. 06-08-00705-a.

Editorial Handling—Dr. A. J. Timothy Jull

REFERENCES

Abdu Y. A. and Ericsson T. 1997. Mössbauer spectroscopy, X-ray diffraction, and electron microprobe analysis of the New Halfa meteorite. *Meteoritics & Planetary Science* 32:373–375.

Abdu Y. A., Ericsson T., Annersten H., Dubrovinskaia N. A., Dubrovinsky L. S., and Gismelseed A. M. 2002. Mössbauer studies on the metallic phases of Al Kidirate and New Halfa meteorites. *Hyperfine Interactions* 5:375–378.

Al-Rawas A. D., Gismelseed A. M., Yousif A. A., Elzain M. E., Worthing M. A., Al-Kathiri A., Gnos E., Hofmann B. A., and Steele D. A. 2007. Studies on Uruq al Hadd meteorite. *Planetary and Space Science* 55:859–863.

Bahgat A. A., Ahmed M. A., Barakat A. A., and Ramadan T. M. 2000. Mössbauer study of El-Bahrain meteorite. *Journal of Radioanalytical and Nuclear Chemistry* 245:615–618.

Bland P. A., Berry F. J., Smith T. B., Skinner S. J., and Pillinger C. T. 1996. The flux of meteorites to the Earth and weathering in hot desert ordinary chondrite finds. *Geochimica et Cosmochimica Acta* 60:2053–2059.

Bland P. A., Kelley S. P., Berry F. J., Cadogan J. M., and Pillinger C. T. 1997. Artificial weathering of the ordinary chondrite Allegan: Implications for the presence of Cl^- as a structural component in akaganeite. *American Mineralogist* 82:1187–1197.

Bland P. A., Berry F. J., and Pillinger C. T. 1998a. Rapid weathering in Holbrook: An iron-57 Mössbauer spectroscopy study. *Meteoritics & Planetary Science* 33:127–129.

Bland P. A., Sexton A. S., Jull A. J. T., Bevan A. W. R., Berry F. J., Thornley D. M., Astin T. R., Britt D. T., and Pillinger C. T. 1998b. Climate and rock weathering: A study of terrestrial age dated ordinary chondritic meteorites from hot desert regions. *Geochimica et Cosmochimica Acta* 62:3169–3184.

Calogero S., Stievano L., and Benoit P. H. 1999. Mössbauer and thermoluminescence studies of meteorites from Frontier Mountain, Antarctica. *Journal of Geophysical Research* 104: 30,817–30,823.

Danon J., Scorzelli R. B., Azevedo I. S., and Michel-Lévy M. C. 1979. Iron-nickel superstructure in metal particles of chondrites. *Nature* 281:469–471.

De Grave E. and Eeckhout S. G. 2003a. Mössbauer studies of some magnetic clinopyroxenes. *Hyperfine Interactions* 148/149:263–274.

De Grave E. and Eeckhout S. G. 2003b. ^{57}Fe Mössbauer-effect studies of Ca-rich, Fe-bearing clinopyroxenes: Part III. Diopside. *American Mineralogist* 88:1145–1152.

De Grave E., Persoons R. M., Vandenberghe R. E., and de Bakker P. M. A. 1993. Mössbauer study of the high-temperature Co substituted magnetites, $Co_\chi Fe_{3-\chi}O_4$. I. $\chi \leq 0.04$. *Physical Review B* 47:5881–5893.

De Oliveira J. C. P., da Costa Jr., M. I., Vasquez A., Roisenberg A., Vieira Jr., N., and Chies J. O. 1988. Mössbauer study of the Putinga chondrite. *Physica Scripta* 37:185–187.

Dodd R. T. 1981. *Meteorites: A petrological-chemical synthesis*. Cambridge: Cambridge University Press. 368 p.

Dunlap R. A. 1997. A Mössbauer effect investigation of the enstatite chondrite from Abee, Canada. *Hyperfine Interactions* 110:209–215.

Dyar M. D., Klima R. L., Lindsley D., and Pieters C. M. 2007. Effects of differential recoil-free fraction on ordering and site occupancies in Mössbauer spectroscopy of orthopyroxenes. *American Mineralogist* 92:424–428.

Eeckhout S. G., De Grave E., McCammon C. A., and Vochten R. 2000. Temperature dependence of the hyperfine parameters of synthetic $P2_1/c$ Mg-Fe clinopyroxenes along the $MgSiO_3$-$FeSiO_3$ join. *American Mineralogist* 85:943–952.

Forder S. D., Bland P. A., Galazka-Friedman J., Urbanski M., Gontarz Z., Milczarek M., and Bakun-Czubarow N. 2001. A Mössbauer study of meteorites—A possible criterion to identify meteorites from the same parent body? *Hyperfine Interactions C* 5:405–408.

Gismelseed A. M., Khangi F., Ibrahim A., Yousif A. A., Worthing M. A., Rais A., Elzain M. E., Brooks C. K., and Sutherland H. H. 1994. Studies of Al Kidirate and Kapoeta meteorites. *Hyperfine Interactions* 91:551–555.

Gismelseed A. M., Worthing M. A., Yousif A. A., Elzain M. E., Al Rawas A. D., and Kamal H. M. 2004. Mineralogical and Mössbauer studies on the paramagnetic separate of Al-Kidirate meteorite. *Physica Status Solidi (a)* 201:482–485.

Gismelseed A. M., Bashir S., Worthing M. A., Yousif A. A., Elzain M. E., AL Rawas A. D., and Widatallah H. M. 2005. Studies and characterizations of the Al Zarnkh meteorite. *Meteoritics & Planetary Science* 40:255–259.

Grandjean F., Long G. J., Hautot D., and Whitney D. L. 1998. A Mössbauer spectral study of the Jilin meteorite. *Hyperfine Interactions* 116:105–115.

Grokhovsky V. I., Oshtrakh M. I., Milder O. B., and Semionkin V. A. 2005a. Mössbauer study of iron meteorites and their corrosion products. *Bulletin of the Russian Academy of Sciences, Physics* 69:1710–1716.

Grokhovsky V. I., Oshtrakh M. I., Milder O. B., and Semionkin V. A. 2005b. Mössbauer spectroscopy of iron meteorite Dronino and products of its corrosion. *Hyperfine Interactions* 166:671–677.

Irkaev S. M., Kupriyanov V. V., Semionkin V. A., and Sokolov M. M. 1987. Method of registration of nuclear γ-resonance. British Patent No. 10745.

Irkaev S. M., Kupriyanov V. V., Semionkin V. A., and Sokolov M. M. 1990. Method of gamma-ray resonance spectroscopy. British Patent No. 2204385.

Jarosewich E. 1990. Chemical analyses of meteorites: A compilation of stony and iron meteorite analyses. *Meteoritics & Planetary Science* 25:323–337.

Kong P. and Ebihara M. 1996. Metal phases of L chondrites: Their formation and evolution in the nebula and in the parent body. *Geochimica et Cosmochimica Acta* 60:2667–2680.

Kong P., Ebihara M., Nagahara H., and Endo K. 1995. Chemical characteristics of metal phases of the Richardton H5 chondrite. *Earth and Planetary Science Letters* 136:407–419.

Kruse O. 1990. Mössbauer and X-ray study of the effects of vacancy concentration in synthetic hexagonal pyrrhotites. *American Mineralogist* 75:755–763.

Leroux H., Doukhan J. -C., and Perron C. 2000. Microstructures of metal grains in ordinary chondrites: Implications for their thermal histories. *Meteoritics & Planetary Science* 35:569–580.

Ludwig A., Zarek W., and Popiel E. 2001. The investigations of chondritic meteorites by X-ray diffraction and Mössbauer effect methods. *Acta Physica Polonica A* 100:761–765.

Malysheva T. V. 1975. *Mössbauer effect in geochemistry and cosmochemistry*. Moscow: Nauka. 166 p.

Menzies O. N., Bland P. A., Berry F. J., and Cressey G. 2005. A Mössbauer spectroscopy and X-ray diffraction study of ordinary chondrites: Quantification of modal mineralogy and implications

for redox conditions during metamorphism. *Meteoritics & Planetary Science* 40:1023–1042.

Migdisova L. F., Zaslavskaya N. I., Ivanov A. V., and Grokhovsky V. I. 1982. Tsarev meteorite: The new shock-metamorphized chondrite (abstract). 13th Lunar and Planetary Science Conference. pp. 518–519.

Morozov M., Brinkmann C., Grodzicki M., Lottermoser W., Tippelt G., Amthauer G., and Kroll H. 2005a. Octahedral cation partitioning in Mg,Fe^{2+}-olivine. Mössbauer spectroscopic study of synthetic $(Mg_{0.5}Fe^{2+}_{0.5})_2SiO_4$ (Fa_{50}). *Hyperfine Interactions* 166:573–578.

Morozov M., Brinkmann C., Lottermoser W., Tippelt G., Amthauer G., and Kroll H. 2005b. Octahedral cation partitioning in Mg,Fe^{2+}-olivine. Mössbauer spectroscopic study of synthetic $(Mg_{0.5}Fe^{2+}_{0.5})_2SiO_4$ (Fa_{50}). *European Journal of Mineralogy* 17: 495–500.

Murad E. and Johnston J. H. 1987. Iron oxides and oxyhydroxides. *Mössbauer spectroscopy applied to inorganic chemistry*, vol. 2, edited by Long G. J. New York: Plenum Publishing. pp. 507–582.

Ortalli I. and Pedrazzi G. 1990. Study of the Torino meteorite. *Hyperfine Interactions* 57:2275–2278.

Oshtrakh M. I. and Zhiganova E. V. 2006. Identification of M1 and M2 sites in olivine and pyroxene by Mössbauer spectroscopy of ordinary chondrites (abstract). *Meteoritics & Planetary Science* 41:A136.

Oshtrakh M. I., Semionkin V. A., Prokopenko P. G., Milder O. B., Livshits A. B., and Kozlov A. A. 2001. Hyperfine interactions in the iron cores from various pharmaceutically important iron-dextran complexes and human ferritin: A comparative study by Mössbauer spectroscopy. *International Journal of Biological Macromolecules* 29:303–314.

Oshtrakh M. I., Milder O. B., Grokhovsky V. I., and Semionkin V. A. 2004. Hyperfine interactions in iron meteorites: Comparative study by Mössbauer spectroscopy. *Hyperfine Interactions* 158: 365–375.

Paliwal B. S., Tripathi R. P., Verma H. C., and Sharma S. K. 2000. Classification of the Didwana-Rajod meteorite: A Mössbauer spectroscopic study. *Meteoritics & Planetary Science* 35:639–642.

Pasternak M. P., Taylor R. D., Jeanloz R., and Bohlen S. R. 1992. Magnetic ordering transition in $Mg_{0.9}Fe_{0.1}SiO_3$ orthopyroxene. *American Mineralogist* 77:901–903.

Scorzelli R. B., Azevedo I. S., and Pereira R. A. 1994. Mössbauer spectroscopy study of the metallic particles extracted from the Antarctic chondrite Allan Hills 769. *Proceedings of the NIPR Symposium on Antarctic Meteorites* 7:299–303.

Scorzelli R. B., Michel-Levy M. C., Gilabert E., Lavielle B., Azevedo I. S., Vieira V. W., Costa T. V. V., and Araujo M. A. B. 1998. The Campos Sales meteorite from Brazil: A lightly shocked L5 chondrite fall. *Meteoritics & Planetary Science* 33: 1335–1337.

Semionkin V. A., Irkaev S. M., Milder O. B., and Oshtrakh M. I. 2005. Methodological features of biomedical application of Mössbauer spectroscopy. *Mössbauer Effect Reference and Data Journal* 28:288–291.

Skinner W. M., Nesbitt H. W., and Pratt A. R. 2004. XPS identification of bulk hole defects and itinerant Fe 3d electrons in natural troilite (FeS). *Geochimica et Cosmochimica Acta* 68:2259–2263.

Solberg T. C. and Burns R. G. 1989. Iron Mössbauer spectral study of weathered Antarctic and SNC meteorites. Proceedings, 19th Lunar and Planetary Science Conference. pp. 313–322.

Sprenkel-Segel E. L. and Hanna S. S. 1964. Mössbauer analysis of iron in stone meteorites. *Geochimica et Cosmochimica Acta* 28: 1913–1931.

Vahonin M. E., Irkaev S. M., Kupriyanov V. V., and Semionkin V. A. 1988a. Spectrometer de Mössbauer. French Patent Fr 2616539-B1, 8708228.

Vahonin M. E., Irkaev S. M., Kupriyanov V. V., and Semionkin V. A. 1988b. Mössbauer spectrometer. British Patent No. 871294.

Van Alboom A., De Grave E., and Vandenberghe R. E. 1993. Study of the temperature dependence of the hyperfine parameters in two orthopyroxenes by ^{57}Fe Mössbauer spectroscopy. *Physics and Chemistry of Minerals* 20:263–275.

Verma H. C., Rawat A., Paliwal B. S., and Tripathi R. P. 2002. Mössbauer spectroscopic studies of an oxidized ordinary chondrite fallen at Itawa-Bhopji, India. *Hyperfine Interactions* 142:643–652.

Verma H. C., Jee K., and Tripathi R. P. 2003. Systematics of Mössbauer absorption areas in ordinary chondrites and applications to newly fallen meteorite in Jodhpur, India. *Meteoritics & Planetary Science* 38:963–967.

Verma H. C. and Tripathi R. P. 2004. Anomalous Mössbauer parameters in the second generation regolith Ghubara meteorite. *Meteoritics & Planetary Science* 39:1755–1759.

Vincze I., Campbell I. A., and Meyer A. J. 1974. Hyperfine field and magnetic moments in b.c.c. Fe-Co and Fe-Ni. *Solid State Communications* 15:1495–1499.

Wang L., Moon N., Zhang Y., Dunham W. R., and Essene E. J. 2005. Fe-Mg order-disorder in orthopyroxenes. *Geochimica et Cosmochimica Acta* 69:5777–5788.

Zhang Y., Stevens J. G., Li Y., and Li Z. 1994. Mössbauer study of the Jilin and Xinyang meteorites. *Hyperfine Interactions* 91: 547–550.

Zhiganova E. V. and Oshtrakh M. I. 2006. Study of metal extracted from Tsarev L5 chondrite by Mössbauer spectroscopy and metallography (abstract). *Meteoritics & Planetary Science* 41: A198.

Zhiganova E. V., Oshtrakh M. I., Milder O. B., Grokhovsky V. I., Semionkin V. A., and Mezentsev A. V. 2005. Mössbauer spectroscopy of ordinary chondrites: An analysis of the metal phases. *Hyperfine Interactions* 166:665–670.

Zhiganova E. V., Grokhovsky V. I., and Oshtrakh M. I. 2007. Study of ordinary chondrites by Mössbauer spectroscopy with high-velocity resolution: Identification of M1 and M2 sites in silicate phases. *Physica Status Solidi (a)* 204:1185–1191.